

# Particle transport analysis of ELMy H-mode pellet fuelled plasma in ASDEX Upgrade

R. Lorenzini\*, P.T. Lang, G. Pereverzev, C.J. Fuchs, J. Stober, ASDEX Upgrade Team

\* *Consorzio RFX, Associazione Euratom-ENEA sulla Fusione, Padova, Italy*  
*Max-Planck-Institut für Plasmaphysik, EURATOM Association, Garching, Germany*

**1. Introduction** The injection of cryogenic fuel pellets from the tokamak high field side allows efficient particle fuelling in hot target plasma. After pellet injection many phenomena take place in the target plasma on different time scales. The pellet ablation and the ablated mass redistribution are followed by a rapid density decrease occurring on a time scale of few milliseconds, which is usually correlated to the presence of strong ELM activity. After these faster phenomena slow diffusion and relaxation of the Post-injection profile take place on the time scale of the order of confinement time (about one hundred milliseconds for ASDEX Upgrade). They are determined by the global transport regime in the target plasma and, from the analysis of this longer phase, transport information can be extracted.

Pellet fuelling experiments of H-mode plasmas have been performed at ASDEX Upgrade during the 2000 campaign with the relevant diagnostics operated in an adapted setting to measure the density profile evolution caused by the pellets with high temporal and spatial resolution. In this paper we present a particle transport analysis for one of the most representative shots in which a train of pellet has been injected from the torus high field side (HFS) in H-mode scenario.

**2. Experimental results** Experiments were performed with the preliminary "looping" injection set up allowing for enhanced pellet launch speed from the HFS [1]. Discharge 14023, chosen for this analysis, has particularly reliable diagnostic data. It is a Hydrogen discharge with low averaged triangularity  $\langle \delta \rangle \approx 0.2$ ,  $B_t = 2.5$  T,  $I_p = 1$  MA. The H-mode confinement is obtained with 6 MW of NBI. After reaching the ELMy H-mode confinement a train of Deuterium pellets, with a repetition rate of 30 Hz and  $v_p = 240$  m/s, has been injected from the HFS.

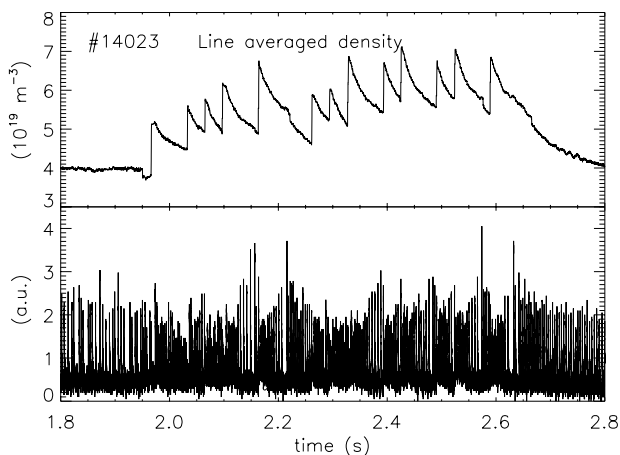


Figure 1: *Density and ELM intensity evolution during the pellet sequence*

During the pellet injection the plasma exhibits an increased ELM activity and the density is characterised by gradual ramp-up, lasting until levelling off point is achieved (Fig.1).

After the launch of the last pellet at  $t = 2.59$  s the density starts decreasing: usually for a few milliseconds the decay is dominated by convective losses related to the presence of strong ELMs [2]; after this fast phenomenon a density decay takes place, which is mainly of diffusive nature. In this discharge the post-pellet decay is not totally diffusive due to a sawtooth event producing a density jump at  $t = 2.665$  s. As shown in Fig. 2 two different

time scales are associated to this diffusive density decay, which is fast over a time interval of

about 100 ms and then slows down.

In this paper we present an evaluation of both the particle diffusion coefficient  $D_H$  which characterises this H-mode plasma before pellet injection and  $D_p$  reproducing the diffusive density decay after the last pellet: the comparison between  $D_H$  and  $D_p$  can give an idea of the effects of this refuelling technique on the plasma confinement.

**3. Simulation results** The tool used for the transport analysis is ASTRA (Automatic System for TRansport Analysis) [3].

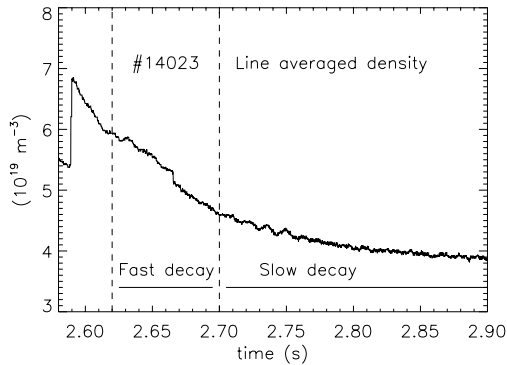


Figure 2: *Density decay after injection of last pellet*

phase after pellet refuelling a data-set of deconvoluted profiles, averaged over 20 ms in the interval between  $t = 2.62$  s and  $t = 2.94$  s has been used. A second data-set of profiles averaged over a shorter time interval (6 ms) was also used to analyse the fast diffusive decay, to control that the longer average time of the first data-set does not affect the results. These density profiles have been compared to those measured by the Thomson scattering system. The two measurements display a good agreement, apart from the central region, where the Thomson scattering yields a higher density. The ECE diagnostic provided the data for electron temperature, and the ion temperature has been set equal to the electron temperature. The analysis skipped 20 ms after the density peaking because of the convective nature of the transport phenomena in this time interval.

Recent results show that the small (2-3 cm/s), inwards directed, neoclassical Ware pinch velocity is a good candidate for reproducing the shape and time scale of density peaking with ICRH and NBI heating when a  $D$  proportional to the experimental energy diffusion coefficient  $\chi$  is used [4]. Therefore we used as particle pinch velocity the Ware pinch in all ASTRA runs. The source term due to neutral influx is calculated assuming scrape-off layer atoms to have a density of  $10^{17} \text{ m}^{-3}$  and a temperature of 3 eV. The contribution of NBI to particle source term has been included as well. ASTRA has been used in interpretative way for calculating the particle diffusion coefficient  $D_H$ ; an analogous run for post-pellet decay showed a diffusivity profile with strong temporal variations, in particular when the data-set of 6 ms averaged profiles is used. In spite of this, the simple assumption of using two different diffusivity profiles,  $D_{p1}$  for the fast density decay phase and  $D_{p2}$  for the slow one, both of them proportional to  $D_H$ , has been adopted. In this way, only one adjustable parameter for each phase was introduced. Despite its simplicity, this approach allows reproducing the shape and the temporal evolution of density

If used in predictive way ASTRA integrates one-dimensional transport equations (e.g. density, electron and ion temperature, magnetic field). This code can be also used in an interpretative way for calculating the transport coefficients from the spatial and temporal evolution of the experimental data. Experimental density profiles are obtained from the deconvolution of interferometry and Li-beam data. The analysis of the phase before pellet injection has been performed on deconvoluted data averaged over 100 ms. For analysing the

profiles and the particle inventory. The resulting profiles, obtained with  $D_{p1} = 1.45D_H$  and  $D_{p2} = 1.1D_H$ , are shown in Fig.3. The corresponding time variation of the volume-averaged density is shown in Fig.4.

The graph on the left in Fig.3 displays two profiles (curves b and c) obtained during the fast decay phase using the  $D_{p1}$  diffusion coefficient. More specifically, curve b is obtained at  $t = 2.67$  s, i.e. in the middle of the fast decay phase, and curve c is obtained at  $t = 2.70$  s, i.e. at the end of the same phase. Curve a shows the initial condition. The pre-pellet profile is also shown (curve e). The matching between the experimental and the computed profiles is good, and the code reproduces very well the decaying temporal evolution. The graph on the right shows two

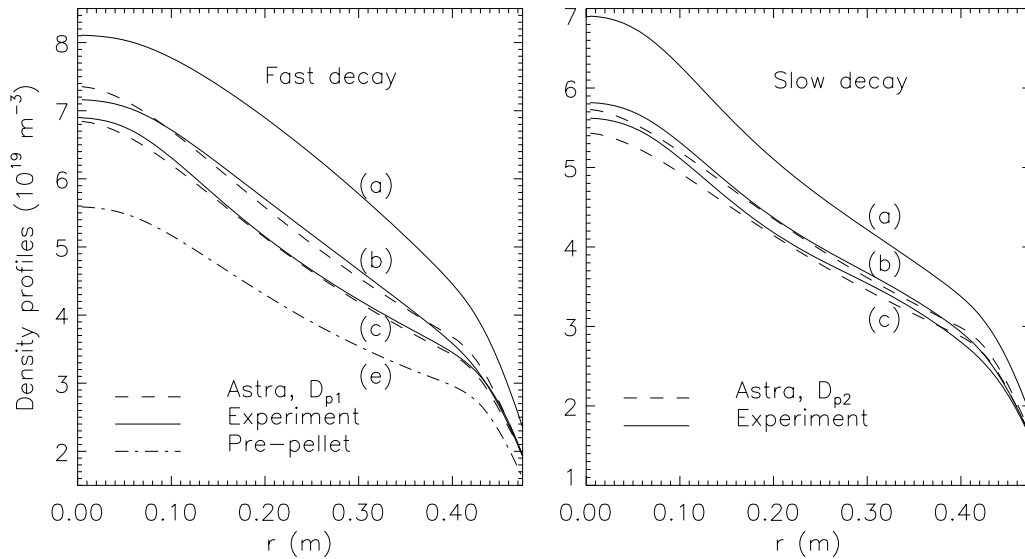


Figure 3: Comparison between calculated and experimental density profiles

profiles (curves b and c) during the slow decay phase. Curve b is obtained at  $t = 2.86$  s, in the middle of the phase, and curve c refers to the last profile of the data-set, at  $t = 2.94$  s. Again, curve a is the initial condition. Also during the slow decay the matching between simulated and experimental profiles is good.

The time evolution of the volume averaged density, shown in Fig. 4, shows an excellent matching between experimental data and simulations, both for the fast decay (left part of the plot) and the slow decay (right part).

The radial profiles of the diffusion coefficients  $D_H$  and  $D_{p1}$  are shown in the top graph of Fig.5. In the bottom graph of the same figure, the coefficients  $D_H$  and  $D_{p2}$  are shown. The shadowed areas indicate the error bars obtained allowing the particle inventory calculated from simulated profiles to differ of 6 % from that obtained with experimental profiles: this amount of uncertainty is used in order to take into account the difference between the particle inventory calculated by means of Thomson Scattering data and the particle inventory calculated by means of deconvoluted profiles and the effect of density decay speeding up due to the sawtooth.

The two curves in the top graph are well separated, even taking into account the error bars, with  $D_{p1}$  larger than  $D_H$ . This implies that in this shot the particle confinement during the fast decay phase was somehow degraded with respect to the pre-pellet phase. On the contrary, although

the diffusion coefficient during the slow decay phase is 10% larger than that in the pre-pellet phase, the error bars superpose.

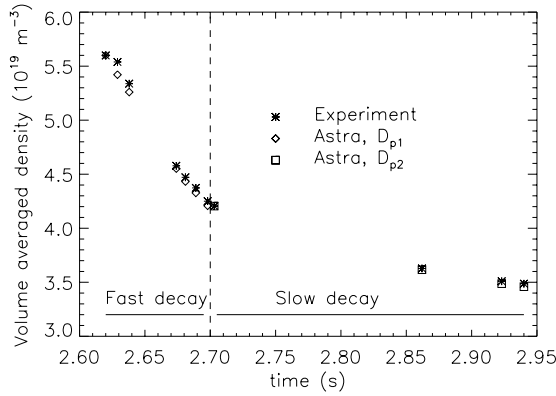


Figure 4: Comparison between experimental and calculated volume averaged density

influx in the post-pellet phase, due to the increased hydrogen outflux driven by the ELM activity. If this effect were taken into account, the diffusion coefficient in the post-pellet phase would be even higher, especially in the edge region. As a consequence, an even larger separation of the two curves in the top part of Fig. 5 would occur.

All the results concerning the fast decay phase obtained using the data-set with profiles averaged over 20 ms have been confirmed by the analysis of the second data-set.

**4. Conclusions** An analysis of particle transport has been performed on a ELMy H-mode discharge refuelled via pellet injection obtained in the ASDEX-Upgrade tokamak.

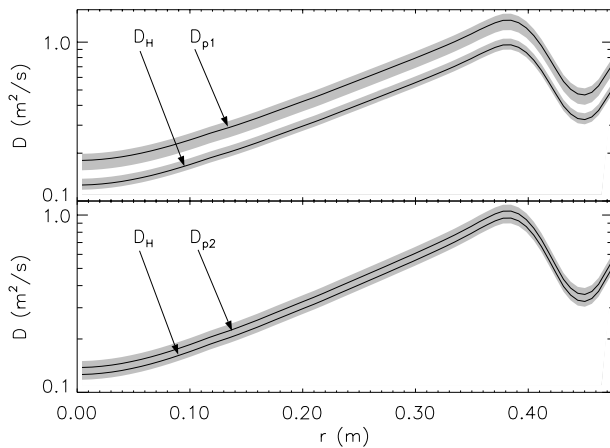


Figure 5: The top and bottom graphs compare respectively  $D_{p1}$  and  $D_{p2}$  to  $D_H$ . The shadowed areas indicate the error bars

- [3] G. Pereverzev et al., IPP 5/42 (1991).
- [4] J. Stober et al., this conference.

Therefore, it is possible to conclude that, given the present measurement precision, the two coincide.

The separation of the two curves in the top part of the figure is present even when the neutral influx is changed by  $\pm 30\%$ , indicating that the result is not strongly sensitive to exact value of this parameter.

It is important to notice that the same value for the neutral influx has been used for the pre-pellet phase and for the two decay phases following the pellet injection. However, it is legitimate to expect an increase of the neutral

influx in the post-pellet phase, due to the increased hydrogen outflux driven by the ELM activity. If this effect were taken into account, the diffusion coefficient in the post-pellet phase would be even higher, especially in the edge region. As a consequence, an even larger separation of the two curves in the top part of Fig. 5 would occur.

All the results concerning the fast decay phase obtained using the data-set with profiles averaged over 20 ms have been confirmed by the analysis of the second data-set.

The simulations show that after the pellet injection an increase in particle diffusivity by a factor of 1.5 is obtained. This increase, which lasts during the first part of the density decay (fast decay), disappears after around 80 ms, when the plasma nearly recovers its original confinement properties at the same density.

**References**

- [1] P.T. Lang et al., "Refueling performance improvement by high speed pellet launch from the magnetic high field side", Nucl. Fusion, in press.
- [2] P.T. Lang et al., Controlled Fusion and Plasma Physics (Proc. 27th Eur. Conf. Budapest, 2000), P3.045.